DOE/NASA/51044-13
NASA TM-81652

Axial Force and Efficiency Tests of Fixed Center Variable Speed Belt Drive

David J. Bents
National Aeronautics and Space Administration
Lewis Research Center

Work performed for
U.S. DEPARTMENT OF ENERGY
Conservation and Solar Energy
Office of Transportation Programs

Prepared for
Society of Automotive Engineers
International Congress and Exposition
Detroit, Michigan, February 23-27, 1981

DOE/NASA/51044-13
NASA TM-81652

Axial Force and Efficiency Tests of Fixed Center Variable Speed Belt Drive

David J. Bents
National Aeronautics and Space Administration
Lewis Research Center
Cleveland, Ohio 44135

Work performed for
U.S. DEPARTMENT OF ENERGY
Conservation and Solar Energy
Office of Transportation Programs
Washington, D.C. 20545
Under Interagency Agreement DE-AI01-77CS51044

Prepared for
Society of Automotive Engineers
International Congress and Exposition
Detroit, Michigan, February 23-27, 1981

TRANSMISSION EFFICIENCY

Transmission efficiency was computed from the measurements in order to gain clearer insight into how it is effected by large increases in belt tension over that which may be required to prevent slippage. For the zero load settings, where the drive is not transmitting an appreciable torque, very little tension is required to keep the belt from slipping and the power losses within the drive should simply increase as the speed or centerline force is raised.

Figure 12 is a plot of power loss versus centerline force computed from the "no load" test data. Since the dynamometer exerted some residual drag torque even when it was not excited, there was a small "output power" which had to be subtracted from the power admitted to the drive. Increases in centerline force tend to cause more work to be done on the belt as it passes into and out of the sheave's (pulley) groove, while increases in speed increase the rate at which this work is done.

The combination of high speeds and small diameters, as evidenced in the speed-up setting, gave the highest power loss.

At settings where torque is transmitted, one would expect higher transmission efficiencies to be observed at low values of the centerline force. The centerline force, which is related to belt tension, should be low enough to not cause excessive deformation work to be done on the belt as it is seated and then unseated from its groove, but should be high enough to prevent the belt from slipping. Transmission efficiency would be high at low centerline force and would decrease as the centerline force is raised.

Figure 13 shows as an example the efficiencies which were observed for the non-zero load test points at unity ratio, 1800 RPM. Each individual test point was computed and plotted versus the centerline force which was created. Efficiencies were calculated as the simple ratio of output power (driven torque x RPM) divided by input power (driver torque x RPM). There is considerable scatter, since this was the ratio of two numbers which were nearly equal

practical design can be established which takes advantage of the rubber belt's unique capabilities without requiring any more space or attention than conventional tranmissions.

The most important element in that practical design is the control system that moves the sheave flanges, which control both speed ratio and belt tension (the sheave assembly, sometimes referred to as a pulley, has a fixed flange and a moveable flange). In order to make a workable control system, the drive has to be characterized; namely, the interactions between moveable flange displacement (drive ratio) and the drive loading, the sheave and belt speeds, and the forces experienced by the drive as power is transmitted must be understood and established in a quantitative fashion. Within the fixed center variable speed belt drives considered for automotive use, we have direct access to three forces -- the axial "sheave spreading" forces on the flange faces arising from the VS belt working in its groove, tending to force open both the driver and driven sheaves, and the "centerline force" which acts to compress the center distance between the shafts closer together as belt tension is increased (fig 1). The centerline force could be considered as the resultant between the axial forces on the sheave flanges and the geometry of the drive, except that this resultant also depends upon how the drive is loaded. These forces are key variables, which can be used to control the drive. The force balance between the driver and driven sheave moveable flanges will determine the actual speed ratio in a running drive while the sum of the forces upon both sheaves, in conjunction with the torgue loading on the drive, will determine belt tension and stress level.

For an automotive CVT the speed ratio must be controlled independent of the speeds and loads the drive is experiencing, and its power transmission efficiency must remain high throughout its useable range of ratio, speeds and loads. Therefore it is essential to know what axial forces will be required to hold the ratio constant at any given condition of speed and load, and how these

axial forces must change as the other conditions are changed. It is also essential to know how the transmission efficiency will vary with the centerline force, or some variable which is related to it directly, so that it may be manipulated in a positive way by the controlled application of axial forces in order to obtain an optimum value for high efficiency, under all conditions within its operating range.

The first characterization that must be performed in order to understand these interactions is the establishment of steady state values for the parameters. This was done experimentally. A test rig, essentially an instrumented VS belt drive CVT driven by a prime mover and connected to an absorbing dynamometer, was designed and built. Fixed, steady-state values of speed ratio, centerline force, and driven sheave (output) speed and torque were run on this rig while measurements were made of the axial forces and input (driver sheave) torque. The resulting data, taken over a carefully chosen range of centerline forces at each selected ratio and power condition, constituted a definitive set of data points within the steady-state operating map of the CVT.

The axial forces which were required to maintain centerline force at each condition, and the drive efficiencies which were observed, are presented as functions of the centerline force at constant (ratio, speed, torque) in order to indicate the magnitude and nature of the data. They are then shown as functions of the V-belt traction coefficient -- a dimensionless variable which is derived from the data.

TEST RIG DESCRIPTION

The test rig was a (double variable sheave) fixed center compound drive connected to a prime mover and power absorber and instrumented to measure the speeds of each sheave, the torques exerted upon them, the centerline force acting between them, and the axial "sheave spreading" forces exerted by the moveable flanges against the belt. The prime

mover/power absorber combination used was an automotive gas turbine engine and its companion dynamometer, located in a test cell at the Chrysler powerplant research laboratory. To convert this installation into a VS belt drive test rig, the long propshaft which normally connects the turbine to the dynamometer was removed, and the fixture shown in fig. 2 was installed between them.

The CVT was basically a symmetrical compound drive with large sheave diameters and short center distance, dimensionally similar to the mechanical torque converters found on snowmobiles. Its dimensions could not be completely duplicated by the test rig due to instrumentation but were similar enough to the CVT to allow controls characterization. These dimensions, which incidentally are almost identical to the Speed Selector model 414 variable speed drive at 42 cm (16 1/2 inch) center distance, are shown in fig. 3.

The test rig fixture was a rigid framework that contained both the apparatus used for test and a toothed cog belt drive, which took the turbine engine's output off center and stepped up the speed. Power was fed to the driver sheave through an inline rotary torquemeter; from there it was delivered back to the absorbing dynamometer through the driven sheave and its connections. The driven center was fixed to the rigid framework, but the driver assembly rode in a swingarm cradle (figure 4) which was also rigid but free to pivot about a spindle parallel to the driven shaft. A load cell, located between the shafts in the plane of the belt and connected to both members through ball-ends, restrained the cradle and sensed the centerline force.

Single-flex gear couplings at each end of the inline torquemeter were used to accomplish a moment-free mechanical connection from the toothed belt drive to the swingarm-mounted driver sheave. A quick-disconnect double-flex gear coupling was used to torsionally connect but otherwise isolate the driven sheave assembly from the dynamometer.

The sheave assemblies (fig. 5) were pneumatically actuated. Each moveable flange rode upon a low-friction ball spline and bushing; actuation air was introduced through a rotary union at the free end of the shaft. Teflon seals were used to reduce air leakage around the actuator cylinder bores, so that the cylinder pressure was essentially the same as the delivery line pressure. Each sheave assembly on its shaft was spin-balanced to 4000 RPM before being installed. The shafts were supported on both ends (as opposed to overhung loading) by lightweight ball bearing pillow blocks.

Figure 6 is a photograph of the test rig installed in the laboratory.

The test rig incorporated measurement of these specific variables, through the following instrumentation:

Driven sheave speed -- The driven sheave assembly was coupled directly to the test cell dynamometer, which has built into it a 60 tooth wheel and magnetic pickup.

Driven sheave torque -- This variable was measured from the dynamometer reaction, which is sensed by a load cell. No provision was made to measure the resistance torque of the driven sheave's shaft support bearings.

Driver sheave speed -- The inline rotary torquemeter included a 60 tooth wheel and magnetic pickup assembly similar to that used by the dynamometer.

Driver sheave torque -- The inline rotary torquemeter, LeBow model 1648, was connected to instrumentation in the control room. No provision was made to measure the resistance torque of the driver sheave's shaft support bearings.

Centerline force -- A load cell, LeBow model 3134, was used. Calibration offsets were used to take into account the dead weight of the belt and driver sheave assembly.

Axial force, driver and driven sheaves -- Actuation air to each sheave assembly was controlled by a hand-adjusted (Norgren model 11-018) pressure regulator which could be set to deliver any gauge pressure between 3.39 kPa (1 in. Hg) and 339 k Pa (100 in. Hg). Piezoelectric pressure transducers (Stratham Labs. model 313) located in each air line immediately upstream of the rotary

unions measured the delivery pressures and transmitted them to the control room. Readings were taken to the nearest 0.34 kPA (0.1 in Hg) and translated by formula to axial force.

An 0.787 mm (0. 031 inch) orifice was inserted in each air line upstream of the transducer, between it and the pressure regulator, to provide actuator damping.

Belt Temperature -- The surface temperature of the moving belt was monitored with an infrared temperature indicator, Raytek model R38A.

The test rig was controlled by operator manipulation of the following variables:

Dynamometer speed -- The dynamometer controller incorporated a servo loop that automatically limits dynamometer speed to an upper bound set by the operator. The dynamometer excitation is modulated by this servo loop normally, within a moderate error, but it can be further modulated by hand for fine corrections, through either the speed setpoint or loop gain, depending upon the degree of precision required. Test points were held within (plus or minus) ten RPM of setpoint, so that in practice there was always a final period of hand tuning after the test point had been initially "roughed in".

Input power -- The automotive gas turbine had several controls which could be used to vary prime mover speed or torque. There were no automatic controls to regulate speed or torque independently but the open loop behavior of the engine was sufficiently stable to let the operator apply input torque corrections as the rig ran.

Sheave pressure -- The set point of each regulator was manually adjusted. The regulator would then hold this pressure automatically. There was no direct control of the moveable flange position. Only the axial forces were controlled. Therefore, the speed ratio could not be set exactly, but had to be achieved and maintained by a dynamic balance of the sheave pressures.

Through manipulation of the dynamometer controls, gas turbine power, and the sheave pressures, the operator would bring the test rig to the desired steady-state condition of constant speed ratio, output speed, output

torque and centerline force. The operator would let the rig stabilize, and then take measurements of all the variables including the sheave pressures which had been used to achieve the condition.

Since it was recognized that small differences in belt construction could exert a major, and unknown, influence on the data, only one particular model of belt was used for all the tests. The test results would probably show influences peculiar to this belt's particular construction, but by using only one belt design this influence would be consistent. The development laboratory of a leading domestic rubber belt manufacturer provided a homogeneous set of experimental belts free-of-charge, with all of the belts made from the same molds and material batch. This belt was representative of the construction considered for an automotive CVT -- raw edge, fabric covered top and molded cog. Its dimensions were nominally equivalent to RMA 3230V570 specification (ref. 1), with a pitchline length of 1448 mm (57 in.), a circumferential length of 1473 mm (58 in.), and a 51 mm (2 in.) top width. Using this belt, the test rig's calculated sheave pitch diameter at unity (one-to-one) drive ratio is 194 mm (7.64 in.).

DESCRIPTION OF TESTS

Test data was taken at three ratios and two speeds; the drive was loaded at two torque levels. Speed, torque, and ratio settings were chosen to differ from one another by a constant factor of 32/18. There were twelve settings in all:

Unity Ratio (one-to-one)

1. 1800 RPM, 0 kW -- output torque = zero
2. 1800 RPM, 8.2 kW -- output torque = 43.4 N-m (32 ft-lb)
3. 1800 RPM, 14.5 kW -- output torque = 77.3 N-m (57 ft-lb)
4. 3200 RPM, 0 kW -- output torque = zero
5. 3200 RPM, 14.5 kW -- output torque = 43.4 N-m (32 ft-lb)

6. 3200 RPM, 25.9 kW -- output
torque = 77.3 N-m (57 ft-lb)
1800/3200 RPM reduction
7. 0 kW -- output
torque = zero
8. 14.5 kW -- output
torque = 77.3 N-m (57 ft-lb)
9. 25.9 kW -- output
torque = 137 N-m (101 ft-lb)
3200/1800 RPM speed-up
10. 0 kW -- output
torque = zero
11. 8.2 kW -- output
torque = 24.4 N-m (18 ft-lb)
12. 14.5 kW -- output
torque = 43.4 N-m (32 ft-lb)

For each of the individual settings, the centerline force was varied in carefully chosen steps from approximately one-and-one-fourth (1-1/4) to ten (10) times the belt tension caused by drive loading alone; this effectively amounted to varying the traction coefficient, which will be explained further in this report, between 0.1 and 0.9. For each no-load setting the centerline force was progresively doubled from 222.4 N (50 lbs.) up to 3560 N (800 lbs). Every non-zero load data point was repeated at least twice during the testing.

TEST SEQUENCE

The data points were run in a sequence which was designed to minimize or limit the fluctuations in test rig and drive belt operating temperature. Data was desired to be steady-state in the thermal sense as well. To do this, the test sequences were arranged so that the total kinetic power within the drive, which is essentially the source of dissipation, was held constant or nearly constant for all adjacent test points. Points of low transmitted power but excessive centerline force were run adjacent to points of more moderate centerline force, but higher transmitted power. In each case the total kinetic power, or the product of belt tensions and pitchline speed, of the next data point would never be appreciably changed from the previous one, but only the external loading and/or speed conditions

which distinguish one setting from another. By changing the kinetic power only incrementally, and by warm-up at the appropriate total kinetic power for 60 minutes or more at the start or each day's testing, it was possible to hold the belt temperatures of repeated data points within five degrees C of each other.

The test matrix was gradually filled in by raising the total kinetic power level and running sequentially all of the individual settings of drive ratio, speed, output torque and centerline force corresponding to that particular kinetic power. When all eight (non-zero load) test settings had been completely covered, the entire test sequence was begun over, beginning with the low total kinetic power points and working upwards. Two repetitions of the sequence were fully completed in this way, and a third partially completed before funding for this project was exhausted. Therefore, because of the way testing was conducted, the time difference between repeated samples is not a matter of minutes but a matter of several weeks.

As a general rule each test point (speed ratio, driven sheave speed and torque, centerline force) took from five to ten minutes to set, and additional ten to twenty minutes to stabilize. Manipulation of the gas turbine controls, dynamometer control and two pressure regulators simultaneously in order to maintain a desired drive condition required considerable activity and skill on the operator's part; each drive condition was the product of a delicate balance of forces and torques. Perturbations in axial force or (prime mover or dynamometer) torque could and often did easily upset this balance, for the drive would respond very quickly to incremental changes. In practice the balance could only be maintained by periodic corrections throughout the test run. Some settings were fairly stable when left to themselves, others were not. Settings which were left unattended over a few minutes time would deteriorate; generally the test rig would slowly drift into extreme speed-up ratio and stay there.

A test point was considered sufficiently stable to record data when no further operator corrections were required within a one minute period, and when the driver pulley speed fluctuations were less than plus or minus ten RPM, evenly centered about the set speed.

TEST RESULTS AND DISCUSSION

The axial force data for each of the twelve settings were compared as a function of the centerline forces which were created. Figure 7 shows an example of that data, corrected for instrument calibration error and translated from pressure measurements to axial force, at unity ratio 1800 RPM. Each plot represents one output (torque) power level. Logarithmic scales are used to compress the region over which data were taken.

The data show scatter, which reflects the conditions which were not controlled during the tests and changed from day to day. These included the test cell ambient air temperature, the humidity inside the test cell, and the changes in the mechanical properties of the belt itself (e.g. bending stiffness, sidewall coefficient of friction) as it deteriorated in service. Short-term scatter could also be attributed to uneven "stiction" between sliding parts of the test rig sheaves. Close repeatability could be obtained if a test point was repeated within a few minutes but not longer time intervals. Because of scatter, the data should be regarded as showing trends only and should not infer absolute levels of performance.

Figure 7a shows that the axial forces on the driver and driven sheaves were equal when no power was transmitted. The centerline force appears as a simple resultant of the axial forces.

When the drive is transmitting power, however, this is no longer true. When load was applied, as figure 7b shows, the driver and driven axial force loci shifted away from each other. As a function of constant centerline force, the driver sheave axial force increased slightly, while the driven sheave axial force decreased. In order to

increase the centerline force at a given transmitted power, and still maintain the same speed ratio, the driver axial force must increase more steeply than the driven axial force. The required difference in axial forces becomes larger as the transmitted torque is increased, as figure 7c shows.

This was also observed earlier by Morgan (ref. 2) and Schlums (ref. 3).

The observations which can be made with figures 7a-7c are illustrated more graphically in figure 8, where trend lines are drawn through the average values of the axial force at each setting, and compiled into one plot which shows all of the unity ratio 1800 RPM axial force trends. For a given centerline force one can compare the differences between unloaded, moderately loaded, and more heavily loaded drives.

As power level is raised, the difference in axial forces become more pronounced. Since the trend lines are nearly parallel, it appears that the axial force difference between the driver and driven sheave depends mainly upon the torque transmitted by the drive and does not depend upon the initial tension. This would agree with the theoretical axial force formulas proposed by Worley (ref. 4).

The axial force behavior of the other nine settings was similar, as can be seen in figures 9, 10, and 11. The force balance shown by the trend lines was influenced by variations in drive loading (torque) more than anything else. There were no significant changes in the force balance with the speed ratio, within the range tested. Because of this, and because of the wide margins of scatter which were observed with the test rig, it is apparent that a VS belt CVT controller that modulates axial force to control speed ratio will have to incorporate some measurement of sheave flange position and close a control loop about this measurement.

A fixed, predetermined pair of constant axial forces will not yield a stable speed ratio. This was also shown by Gerbert's analysis (ref. 5).

TRANSMISSION EFFICIENCY

Transmission efficiency was computed from the measurements in order to gain clearer insight into how it is effected by large increases in belt tension over that which may be required to prevent slippage. For the zero load settings, where the drive is not transmitting an appreciable torque, very little tension is required to keep the belt from slipping and the power losses within the drive should simply increase as the speed or centerline force is raised.

Figure 12 is a plot of power loss versus centerline force computed from the "no load" test data. Since the dynamometer exerted some residual drag torque even when it was not excited, there was a small "output power" which had to be subtracted from the power admitted to the drive. Increases in centerline force tend to cause more work to be done on the belt as it passes into and out of the sheave's (pulley) groove, while increases in speed increase the rate at which this work is done.

The combination of high speeds and small diameters, as evidenced in the speed-up setting, gave the highest power loss.

At settings where torque is transmitted, one would expect higher transmission efficiencies to be observed at low values of the centerline force. The centerline force, which is related to belt tension, should be low enough to not cause excessive deformation work to be done on the belt as it is seated and then unseated from its groove, but should be high enough to prevent the belt from slipping. Transmission efficiency would be high at low centerline force and would decrease as the centerline force is raised.

Figure 13 shows as an example the efficiencies which were observed for the non-zero load test points at unity ratio, 1800 RPM. Each individual test point was computed and plotted versus the centerline force which was created. Efficiencies were calculated as the simple ratio of output power (driven torque x RPM) divided by input power (driver torque x RPM). There is considerable scatter, since this was the ratio of two numbers which were nearly equal

to each other. Small errors in either number caused larger errors in the ratio. Despite the scatter, however, it can be seen that the range of observed efficiencies fell into the mid-nineties, and that efficiency decreased as the centerline force was raised.

The same trends were evident with the other nine settings. The efficiency calculations had no corrections applied for bearing or windage loss. The test rig data was used directly.

TRACTION COEFFICIENT

When examining belt drive data which were measured over a wide range of loads and applied forces at the different speeds and ratios, it is helpful to consider an analysis variable which can translate the interaction of torques, tensions, and forces being applied to the drive into a single quantity that expresses directly how heavily the drive is loaded. This variable was first defined by B. G. Gerbert (ref 5), who named it "traction coefficient" and gave it the symbol lambda (λ). It is defined as the ratio of the difference between the tight side belt tension and the slack side tension divided by the sum of the tight and slack side tensions:

Traction Coefficient $$\lambda = \frac{t_1 - t_2}{t_1 + t_2}$$

This variable is related to the more familiar "tension ratio" t_1/t_2 by the relation:

$$\lambda = \frac{(t_{1/t_2}) - 1}{(t_{1/t_2}) + 1}$$

A traction coefficient of zero indicates a drive which is not transmitting torque, no matter how high the individual belt tensions are. At the other extreme is a unity traction coefficient, which never occurs because it is equivalent to zero slack side tension; all of the tension in the drive being used to transmit torque. Actual traction coefficients lie somewhere between zero and one.

The traction coefficients were derived from the test data by simple formulas. More precise determination of the traction coefficient and belt tensions, which rely upon measurements unavailable on this test rig (such as the actual pitch diameter, for example) were not considered to be of any additional benefit since their improved precision would be superfluous. The tension sum of the tight and slack side belt tensions was computed from the centerline force by simple geometry correction:

$$\text{Tension Sum } t_1 + t_2 = \frac{CF}{\sqrt{1 - \left(\frac{D_{11}\left(\left(\frac{TdR}{TdN}\right) - 1\right)}{CD\left(\left(\frac{TdR}{TdN}\right) + 1\right)}\right)^2}}$$

The tension difference between the tight and slack sides, which is directly related to the pulley torque, was computed as the average:

$$\text{Tension difference } t_1 - t_2 = \frac{TdR + TdN}{D_{11}}$$

We can use the traction coefficient to show how much of the total kinetic power within the drive is transmitted. The kinetic power is the sum of the products of belt tension and pitchline speed, namely:

kinetic power = $(t_1 + t_2)$ x (belt pitchline speed)

The total kinetic power is always larger than the transmitted power due to nonzero slack side tension. If λ is zero, the tight and slack side tensions are equal and none of the kinetic power is transmitted. If it is nonzero there is a difference between the tight and slack side tensions and therefore a fraction of the kinetic power, a fraction essentially equal to λ, will be transmitted. Since the loss mechanisms at work within the drive are taxing the total kinetic power, not the transmitted power, it seems advantageous to operate at higher values of λ.

Low values of λ imply large amounts of total kinetic power built up within the drive, compared with the useful power being passed through. The centerline force and tension is excessive. Higher values of imply a greater fraction of the kinetic power being transmitted so that, up to a point, the tax on the drive's transmitted power is reduced. If we were to plot the transmission efficiency of the belt drive against the traction coefficient, at any speed or power level, we should observe low efficiencies at near-zero values of λ, increases in the efficiency as λ tended towards one, and a maximum value near the highest λ that can be reached before the belt begins to slip. Beyond this maximum, we should observe a sharp drop in efficiency.

Figures 14a through 14d are plots of the averaged transmission efficiencies for the different settings, shown as functions of the traction coefficient rather than the centerline force. Since the traction coefficient is an expression of transmitted power, the test settings of a given speed and drive ratio can be combined. Note that the overdrive setting shows the most loss and behaves most nearly according to prediction. The efficiencies of all the settings are increased as the traction coefficient moves away from the zero. When λ is reasonably constrained between .3 and .6, the efficiency appears to reach a maximum.

The efficiency values are somewhat higher than those recorded by Palmer and Bear (ref. 6) on a smaller VS belt drive.

A clearer picture of the drive's axial force behavior might also be obtained if this quantity were expressed as a function of the traction coefficient. In order to compress the data into a more concise form without using the logarithmic scale we can also normalize the axial forces to the belt tension sum, since axial force increases almost directly with the tensions:

$$\text{Normalized Axial Force} = \frac{F_z}{t_1 + t_2}$$

and show the generalized axial force

behavior which was observed on the test rig as a function of the traction coefficient.

Figure 15 is B. G. Gerbert's prediction (ref. 5) of the normalized axial force versus traction coefficient for a fixed center variable speed belt drive similar to the geometry of the test rig. According to the prediction, the driven sheave normalized axial force should remain almost constant with traction coefficient, while the driver normalized axial force should increase at a near constant rate. As speed ratio changes, the slope of this increase should also change.

Figures 16a through 16d are averaged and normalized plots of the axial force data previously presented in figures 8 through 11 now shown as functions of the traction coefficient. For each speed and speed ratio setting, data taken at different power levels can now be combined since these points will lie on the same curve.

The data fall into the same range of magnitudes, and exhibits similar trends to the predictions of figure 15. It is not apparent from the tests, however, that axial forces are influenced by speed ratio in exactly the manner predicted. The problem remains one of the isolating more of the mechanisms at work in the actual drive, which are not accounted for or described by the present theory, but which might explain the scatter which was observed and better link the data to a smooth theoretical curve.

CONCLUSIONS

From the data these general observations can be validated:

1. The axial force behavior of the fixed center variable speed belt drive, measured experimentally, agrees reasonably well with theoretical predictions but does not follow them exactly.
2. Changes in the axial force that is required to balance variations in the applied torque are much greater than changes due only to speed or ratio variation.

3. Transmission efficiency of the drive is high, over wide variations in load. It is maximized by maintaining the traction ratio, or the belt tensions and centerline force, within moderate limits.

ACKNOWLEDGEMENTS

The author wishes to express his appreciation to these organizations and persons who contributed freely of their resources, time, talent and experience:

The NASA Electric Venicle Systems Project Office through which Department of Energy funds were provided for the tests.

Mr. Bruce Chapman and Mr. Chris Mader of Chrylser, who looked after the test rig and kept it running.

For their critical review and comment on this work I wish to thank Dr. Larry Oliver of DAYCO for his encouragement, support, and enthusiasm and also Mr. W. Spencer Worley of Gates Rubber for his insight and many helpful suggestions.

REFERENCES

1. RMA Engineering Standard "Specification for Drives Using Variable Speed V-belts." Rubber Manufacturers Association, New York, November 1966, revised January 1971.
2. N. E. Morgan, "Experimental Data Disagree with Theoretical Results." discussion of (3), SAE Transactions, Vol. 63, 1955, pp. 330-331.
3. W. S. Worley, "Designing Adjustable Speed V-belt Drives for Farm Implements." SAE Transactions, Vol. 63, 1955, pp. 321-330.
4. K. D. Schlums, "Equations of Forces and Motion of Power Transmission Mediums in V-shaped Pulleys." Journal of Mechanisms, Vol. 2, 1967, pp. 395-406.
5. B. G. Gerbert, "Adjustable Speed V-belt Drives -- Mechanical Properties and Design." SAE Paper 740747, 1974.
6. R. S. J. Palmer and J. H. F. Bear, "Mechanical Efficiency of a Variable-Speed, Fixed Center, V-belt Drive." Journal of Engineering For Industry, Vol. 99, August 1977, pp. 806-808.

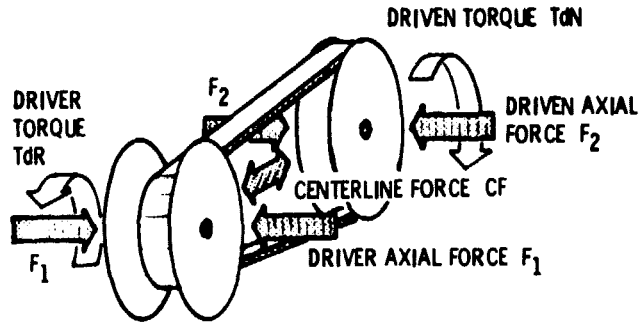

Figure 1. - Force balance in fixed center vs. belt drive.

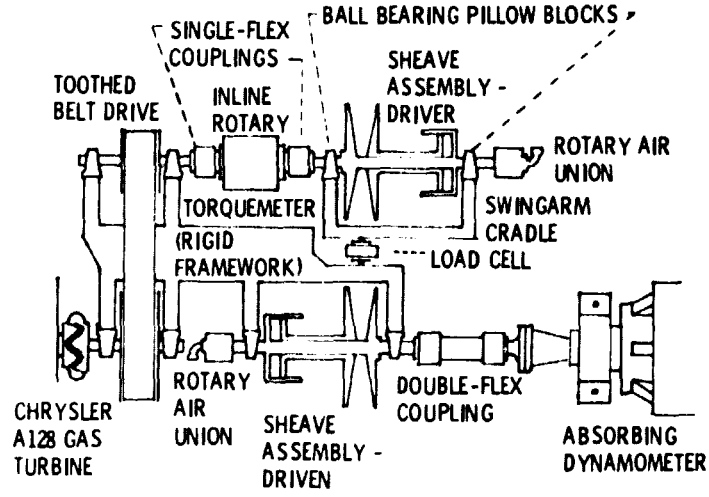

Figure 2. - VS Belt drive axial force test rig.

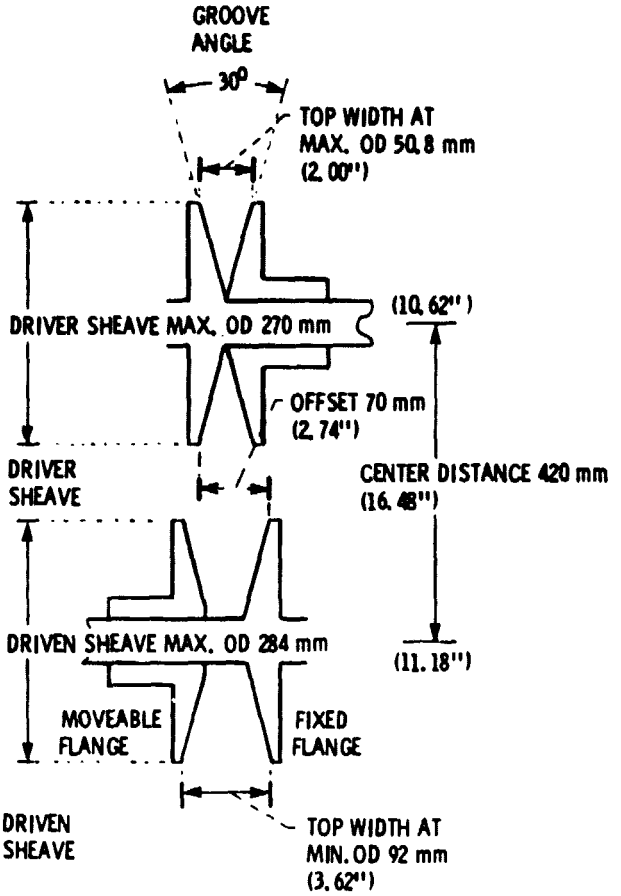

Figure 3. - Test rig dimensions.

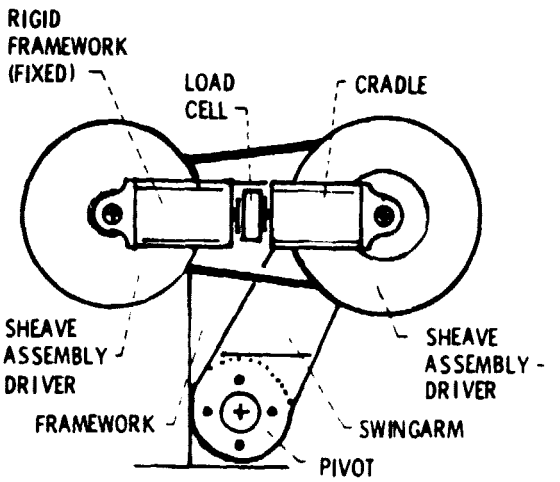

Figure 4. - Test rig detail - swingarm cradle (looking forward from dynamometer).

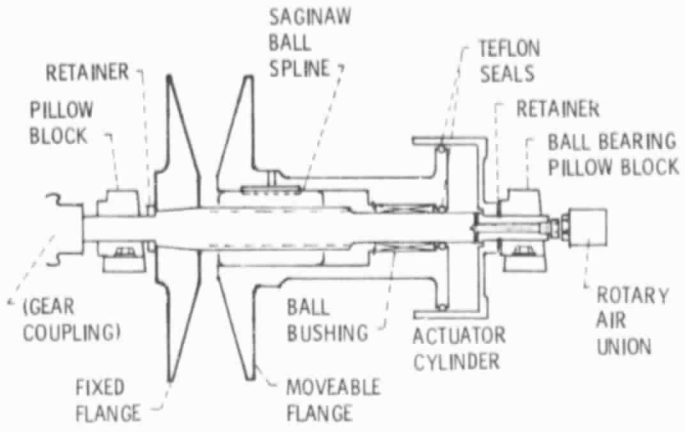

Figure 5. - Test rig detail - sheave assembly.

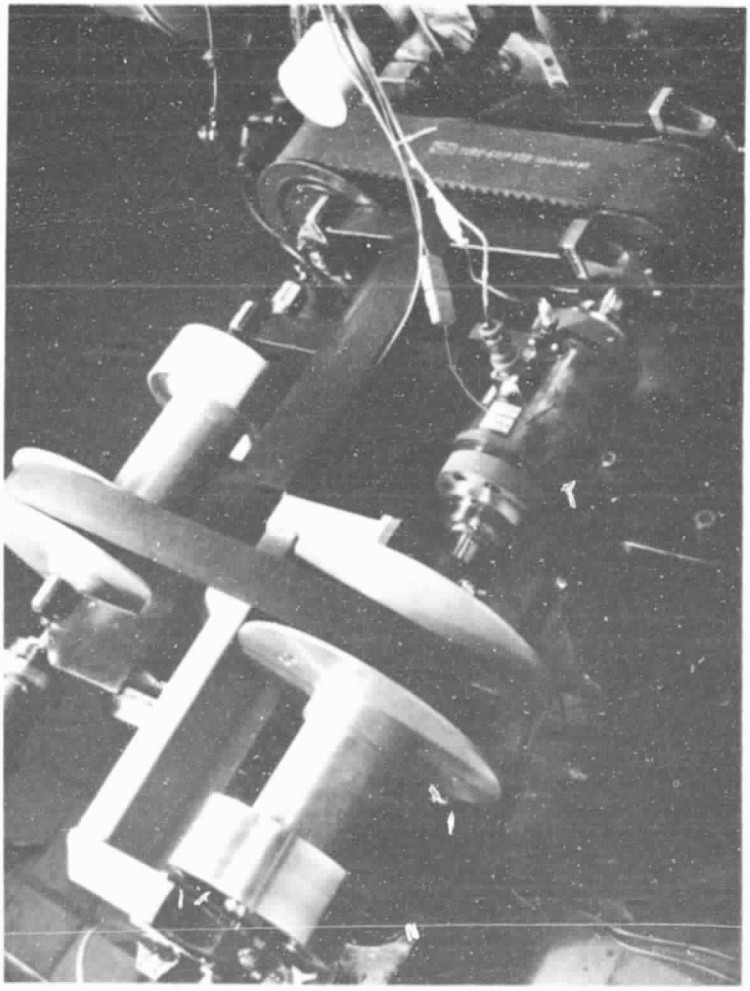

Figure 6. - Test rig installation.

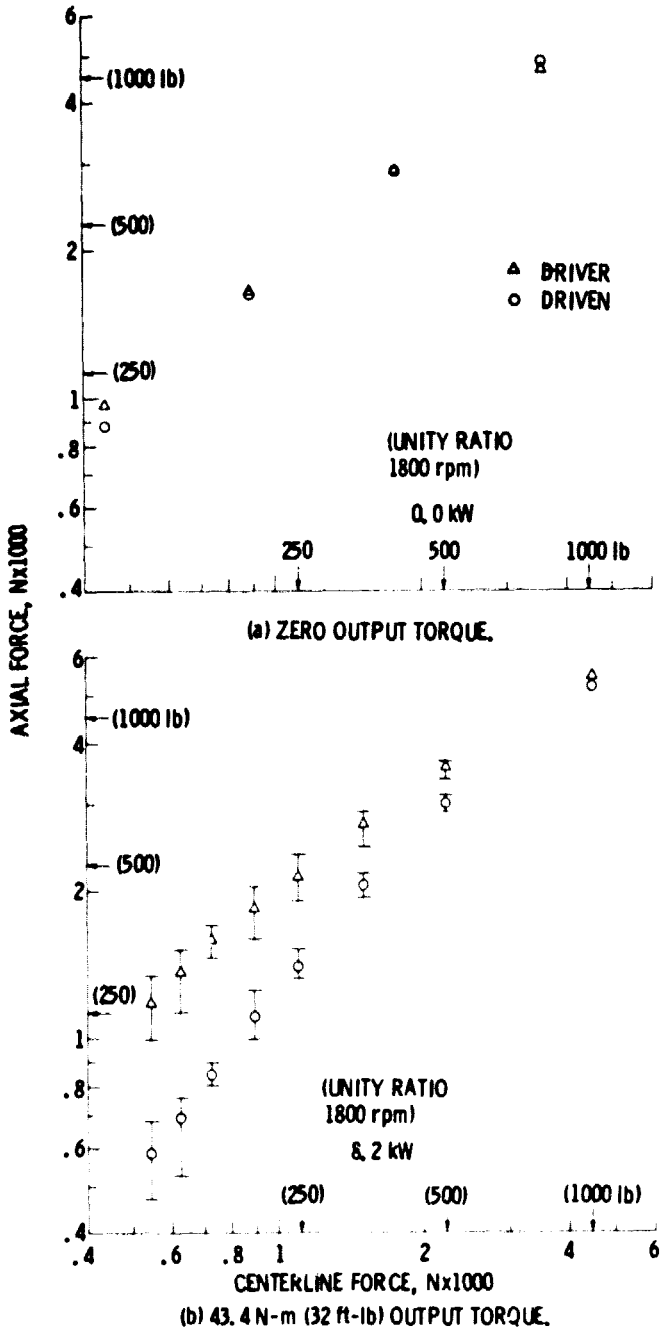

Figure 7. - Data - Axial force versus centerline force at constant speed and output torque, unity ratio 1800 rpm.

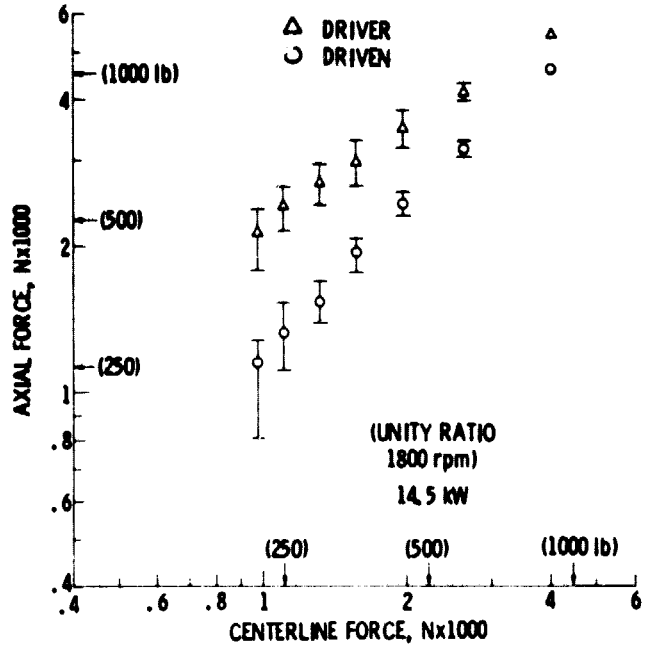

(c) 77.3 N-m (57 ft-lb) OUTPUT TORQUE.

Figure 7. - Concluded.

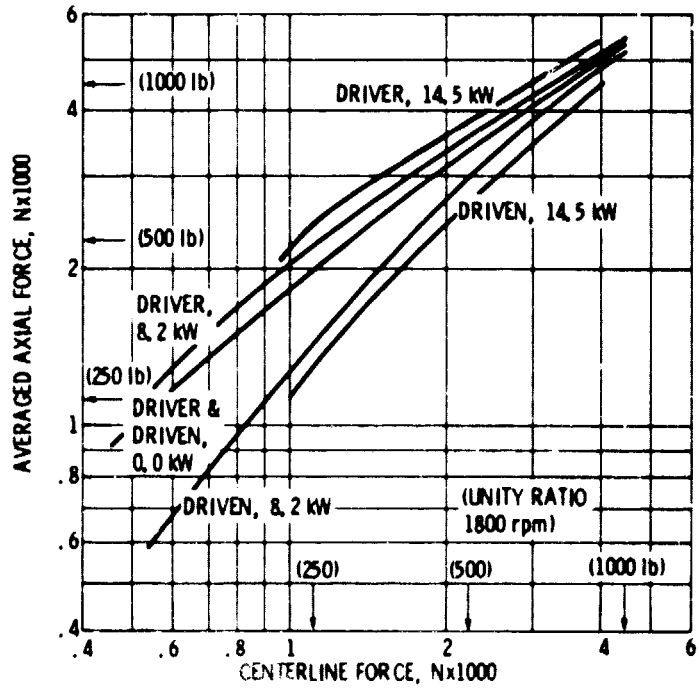

Figure 8. - Averaged axial force versus centerline force, all unity ratio 1800 rpm settings.

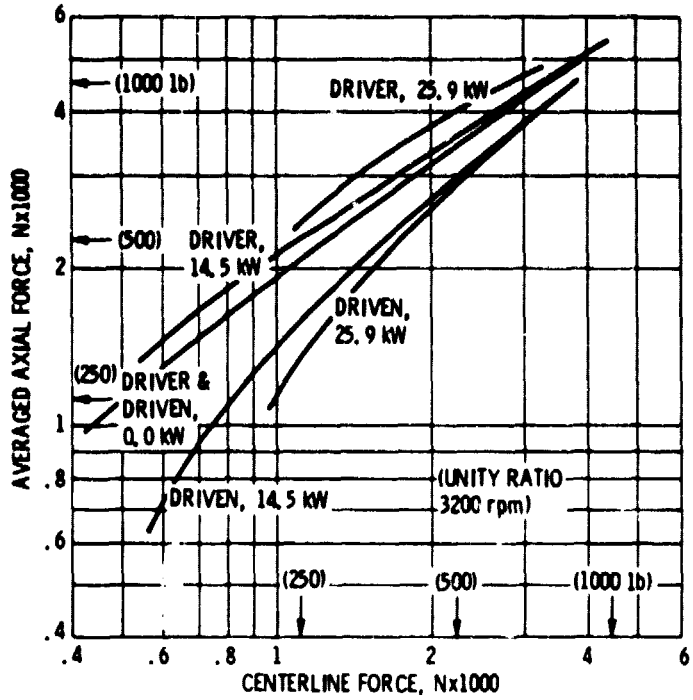

Figure 9. - Averaged axial force versus centerline force, all unity ratio 3200 rpm settings.

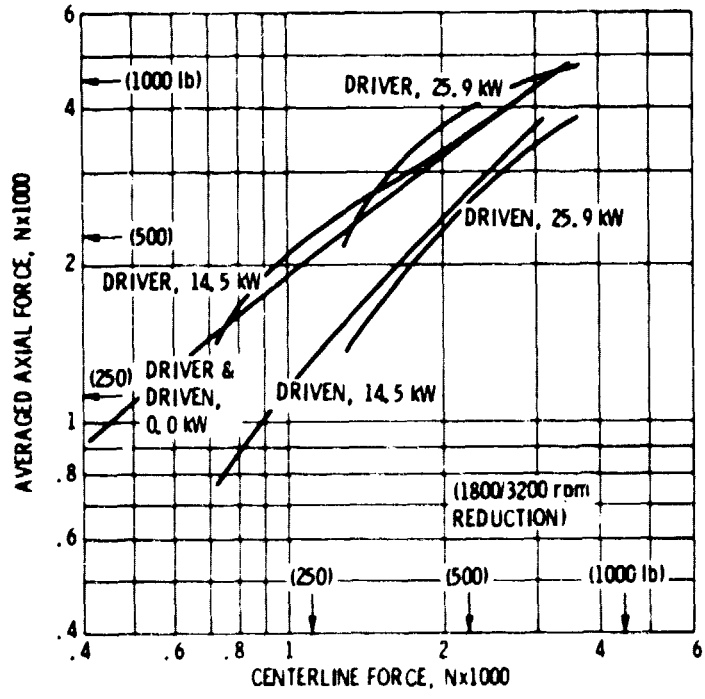

Figure 10. - Averaged axial force versus centerline force, all 1800/3200 rpm reduction settings.

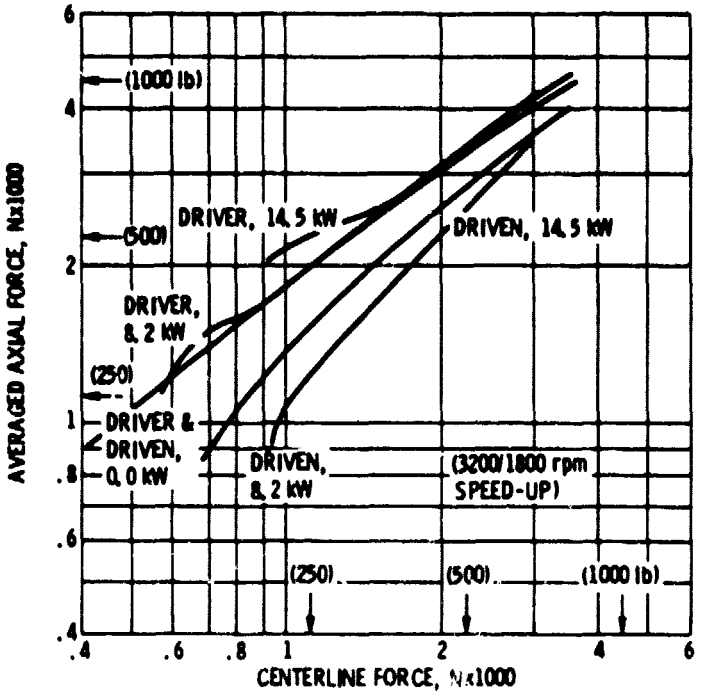

Figure 11. - Averaged axial force versus centerline force, all 3200/1800 rpm speed-up settings.

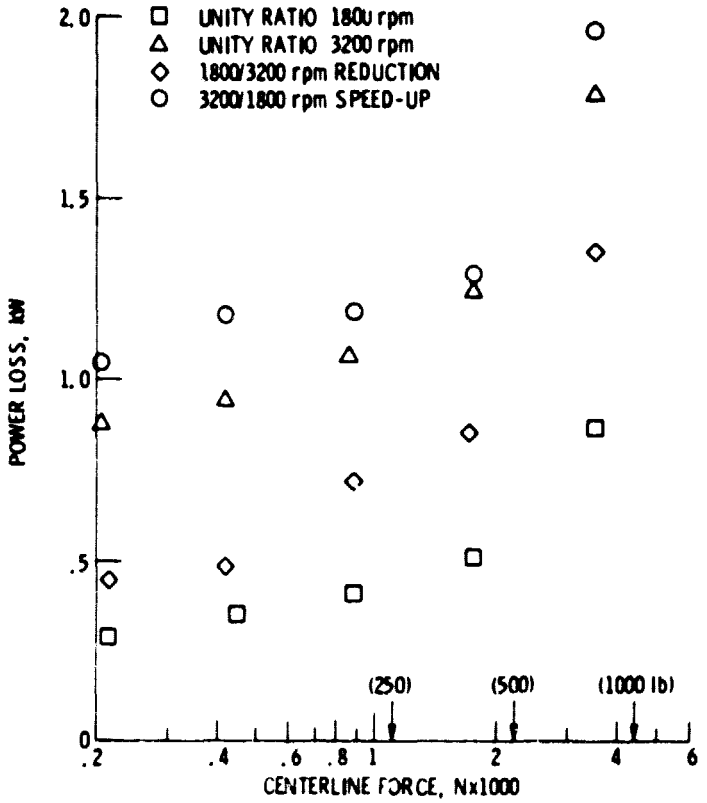

Figure 12. - Data - no-load power loss versus centerline force.

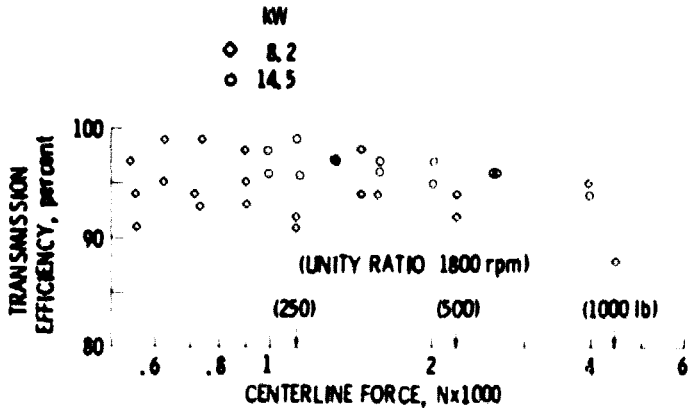

Figure 13. - Data - efficiency versus centerline force, unity ratio 1800 rpm.

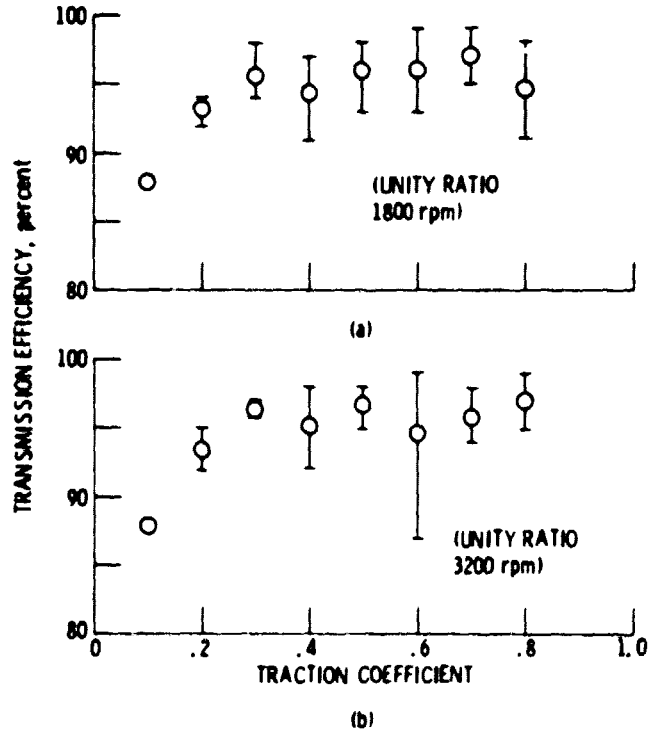

Figure 14. - Efficiency (average) versus traction coefficient.

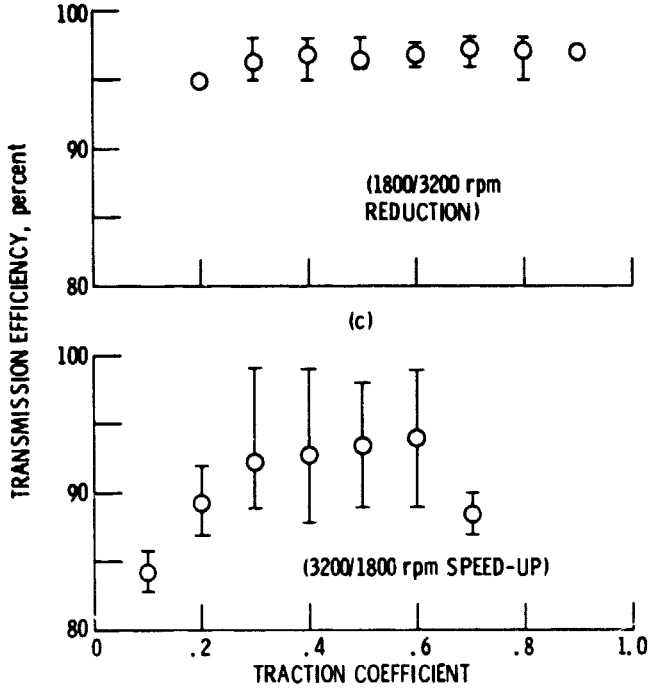

Figure 14. - Concluded.

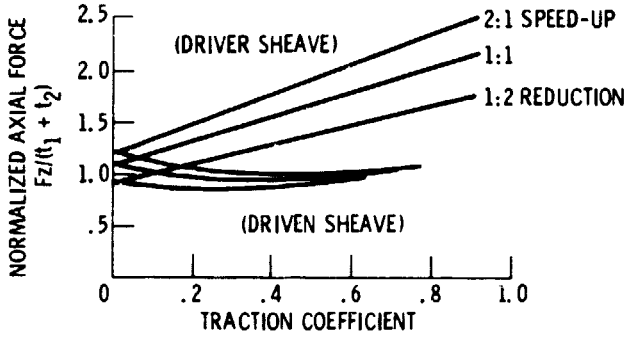

Figure 15. - Normalized axial force as a function of the traction coefficient, predicted by B. G. Gerbert (ref. 5).

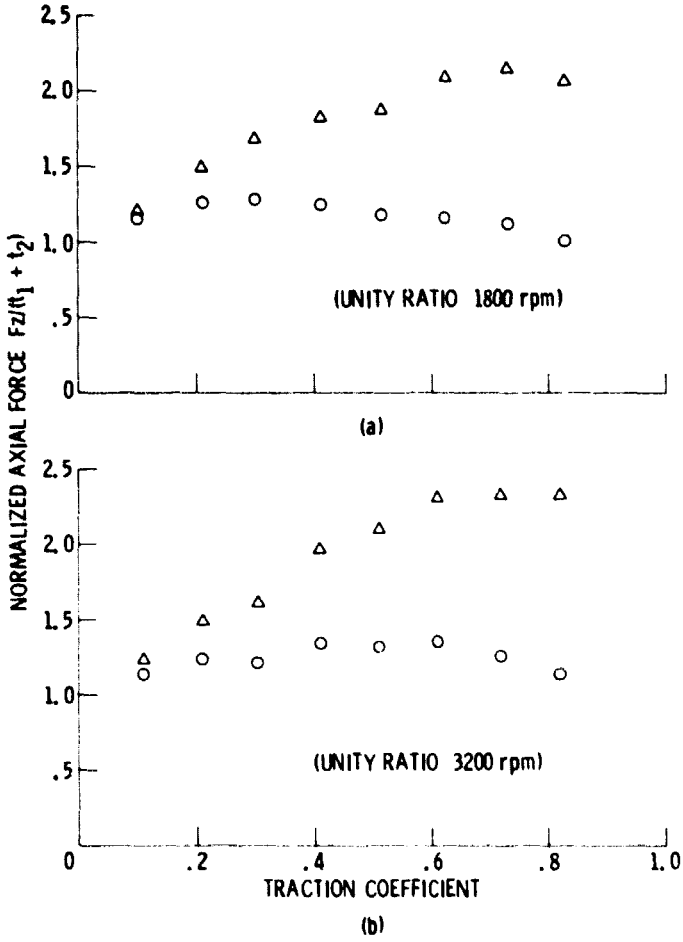

Figure 16. - Data - normalized axial force versus traction coefficient.

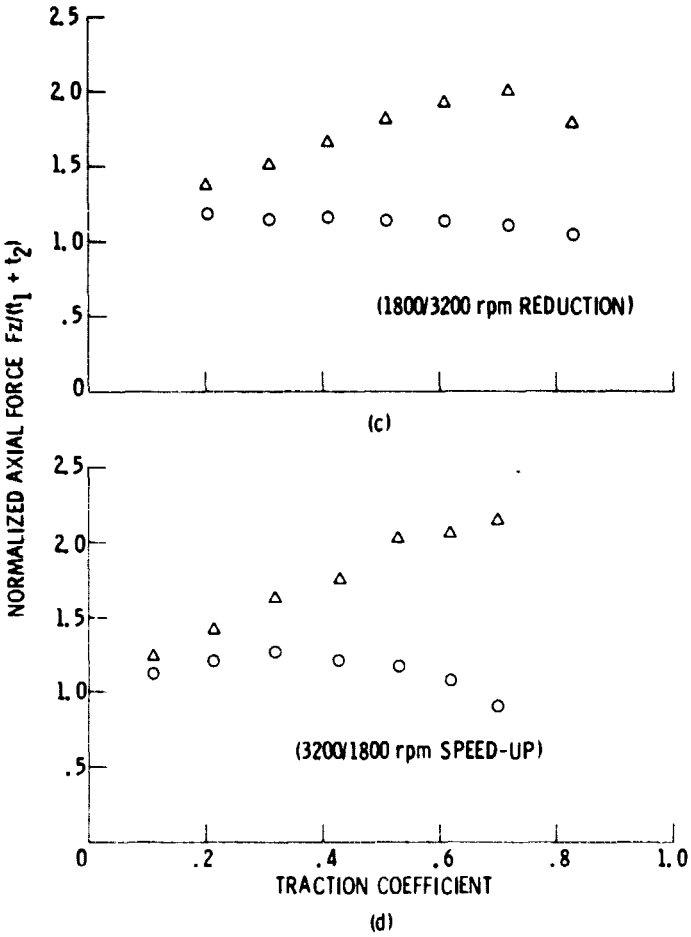

Figure 16. - Concluded.